

INTRODUCTION

The State of Nevada occupies most of the central and western parts of the Great Basin, the largest tectonically active region within the Basin and Range geomorphic province of North America. The topography of this region is typified by generally north-northwest- to northeast-trending, subparallel mountain ranges separated by alluvial basins of similar plan form and orientation. This classic Basin and Range physiography is the product of at least two phases of middle to late Cenozoic extensional faulting (Zoback and others, 1981; Eaton, 1982; Stewart, 1983), and most of the basins and ranges of the region are at least partly bounded by late Cenozoic faults. The earlier phase of extension was marked by widespread basement faulting that began at approximately 35 Ma and locally continued into the time of the later phase (Eaton, 1982; Stewart, 1983). The later phase, which was dominated by high-angle, more deeply penetrating block faulting, may have begun locally at about 17 Ma and continues episodically to the present time (Christiansen and McKee, 1978; Eaton, 1982). This map, one of a series of 1° by 2° quadrangle maps showing young faults in Nevada, provides a generalized picture of the late Tertiary and Quaternary faulting that is associated with the later extensional phase. These young faults are a primary determinant of the present configuration of ranges and basins within the quadrangle.

MAPPING PROCEDURE

Young faults are herein defined as those faults that have undergone latest Tertiary and (or) Quaternary movement. These faults are commonly marked by a variety of diagnostic structural landforms and other surficial phenomena that can be readily identified and mapped on aerial photographs. These features include (1) scarps on latest Tertiary and (or) Quaternary surficial deposits, volcanic or geomorphic surfaces (either erosional or depositional); (2) prominent alignments of linear drainages, ridges and swales, active springs and (or) spring deposits, and linear discontinuities of structure, rock type, and vegetation; and (3) abrupt, steeply sloping range fronts with well-defined, faceted spurs, wingless valleys, and elongate drainage basins with narrow valley floors (Thornbury, 1969; Bull, 1977; Bull and McFadden, 1977; Wallace, 1977, 1978).

National High Altitude Program (NHAP), 1:58,000 nominal-scale, color-infrared topographic map was used for photogeologic interpretation. This mapping was transferred directly to 1/2° by 1° topographic quadrangle maps that were enlarged to the scale of the photographs. These maps were reduced and compiled at 1:250,000 scale. This compilation was then compared with previous mapping of young faults within the quadrangle (Ertex Western, Inc., 1981; see fig. 1; Barnhard, 1985) and significant differences between maps were resolved. Because this previous mapping included extensive field verification, more young faults were identified by this mapping than by the present reconnaissance study. Many of these additional faults are located on distal piedmonts and basin flats and most are included on our map.

Following comparison and resolution with previous mapping, the final 1:250,000-scale compilation was digitized using a GTECO digitizing board connected to a Macintosh II microcomputer. The resulting vector file was converted to raster (500 m cell size) and analyzed to determine the approximate length and average orientation of each fault segment. These data are summarized in table 1 and figure 2.

General ages of surficial deposits and geomorphic criteria used to estimate ages were estimated using a variety of photogeologic and geomorphic criteria (table 2). These age estimates provide a general indication of the approximate timing of young faulting throughout the quadrangle. However, it should be emphasized that these data do not necessarily reflect the age of most recent surface rupture along any particular fault segment. Rather, they provide a very general (and commonly somewhat biased) age constraints on this surface faulting. Age estimates based on photogeologic analysis of surficial deposits and erosion surfaces are, at best, both tentative and imprecise. Moreover, the distribution of these deposits and surfaces is inherently biased by geomorphic process and environment. For example, in those areas of the Great Basin where range width rates are low to moderate, remnants of older geomorphic surfaces tend to be concentrated in proximal piedmont areas, whereas younger surficial deposits tend to accumulate on distal piedmonts and basin flats. Consequently, young faults located in intrabasin areas are more likely to offset younger surface deposits than are faults located along range fronts or in proximal piedmont areas. Therefore, inferences based on these data regarding the temporal distribution of young fault activity should be used with caution.

In addition to the limitations imposed by map and photo scales, one other factor also significantly constrains the resolution of the present map. The photography used in this analysis, which was acquired under high sun-angle conditions, is not well suited for the discrimination and mapping of subtle topographic features. Consequently, reexamination of any of the fault systems shown on this map using larger scale and (or) lower sun-angle aerial photography would very likely reveal a substantial number of additional young fault segments.

PATTERNS OF LATEST TERTIARY AND QUATERNARY FAULTING

Several factors significantly influence the preservation of fault-related landforms and, therefore, the apparent distribution of young faults as indicated by the distribution of these landforms can be significantly biased. These factors include (1) composition, inclination, and structural integrity of the rock or sediment type(s) underlying fault scarps; (2) local geomorphic environment of the scarp or other fault-related landforms; (3) regional climatic conditions and paleoclimatic variations; and (4) magnitude and recurrence of fault movement (Wallace, 1977; Bucknam and Anderson, 1979; Nash, 1984; Hanks and others, 1984; Mayer, 1984; Pierce and Colman, 1986; Machette, 1986, 1988, 1989). Therefore, the distribution of young faults shown on this map provides, at best, only an approximate and somewhat biased picture of late Tertiary and Quaternary faulting within the quadrangle. Specifically, faults having a long history of recurrent movement, juxtaposing bedrock and alluvium, or cutting upper Cenozoic lava flows and (or) welded ash flow tuffs tend to be overrepresented whereas faults of pre-late Pleistocene age cutting unconsolidated surficial deposits and having either short histories of recurrent movement or long recurrence intervals tend to be underrepresented. Scarps developed on volcanic rocks may be preserved for periods of as much as 10 m.y. By comparison, scarps on the fluvially active parts of piedmont surfaces would likely be completely destroyed within a few thousand years at most, and even on inactive piedmont surfaces, fault scarps on unconsolidated alluvial fill are significantly rounded within 10,000 years (Wallace, 1977), and low scarps would be sufficiently degraded to be unrecognizable on standard aerial photography within a few hundred thousand years (Wallace, 1977; Hanks and others, 1984; Machette, 1989).

The density and orientation of young faulting in the Elko 1° by 2° quadrangle are fairly typical of the Great Basin. Fault orientations are predominantly north-northeasterly in areas to the west of Ruby Valley, whereas they are predominantly northerly in areas to the east of that valley (table 1; fig. 2). This west-to-east change in orientation is part of a general change in young fault orientation across the central Great Basin from central Nevada to central Utah. Relatively little young faulting is present in the east central and extreme northwestern parts of the quadrangle. However, young faults are relatively uniformly distributed across the remainder of the map area where average young fault densities range between 0.05 and 0.07 km/km<sup>2</sup> (table 1).

Nearly continuous range-front faults bound (1) the west flanks of the East Humboldt Range, Spruce Mountain Range, the Peapack Mountains, and the Mawick Spring Range; (2) both the east and northwest flanks of the Ruby Mountains; and (3) the east flank of the Cherry Creek Range. However, young range-front faulting is conspicuously absent along most of the length of the Goshute Range in the east-central part of the quadrangle. The fault along the Cherry Creek Range is the northern continuation of a major range-front fault zone that bounds the east side of the Egan Range in the Ely 1° by 2° quadrangle to the south. This fault zone is nearly 160 km long and one of the longest in the central Great Basin. Major range-front fault zones showing evidence of substantial late Pleistocene and (or) Holocene movement are located along the Ruby Mountains and (or) Holocene movement are located along the northwest flank of the Mawick Spring Range just east of Ruby Lake and along the east flank of the Antelope Range and the Kingsley Mountains in the southeast corner of the quadrangle. Faults of probable Holocene age are located in the south end of Huntington Valley, the west central part of Ruby Valley, and the north end of Steptoe Valley.

REFERENCES CITED

Barnhard, T.P., 1985, Map of fault scarps formed in unconsolidated sediments, Elko 1° x 2° quadrangle, Nevada and Utah: U.S. Geological Survey Miscellaneous Field Studies Map MF-1791, scale 1:250,000.  
Bucknam, R.C., and Anderson, E.C., 1979, Estimation of fault-scarp ages from a scarp-height-slope-angle relationship: *Geology*, v. 7, p. 11-14.  
Bull, W.B., 1977, Tectonic geomorphology of the Mojave Desert, California: U.S. Geological Survey, Office of Earthquakes, Volcanoes, and Engineering, Contract Report 14-08-001-G-394, Menlo Park, Calif., 188 p.  
Bull, W.B., and McFadden, L.D., 1977, Tectonic geomorphology north and south of the Garlock fault, California, in Drexler, D.C., ed., *Geomorphology in arid regions: Proceedings 8th Annual Geomorphology Symposium*, State University of New York, Binghamton, p. 115-137.  
Christiansen, R.L., and McKee, E.H., 1978, Late Cenozoic volcanic and tectonic evolution of the Great Basin and Columbia intermontane basins: *Geological Society of America Memoir* 182, p. 283-311.  
Eaton, G.P., 1982, The Basin and Range Province: Origin and tectonic significance: *Annual Reviews Earth and Planetary Science*, v. 10, p. 409-440.  
Ertex Western, Inc., 1981, Faults and lineaments in the MX siting region, Nevada and Utah: unpublished report prepared for the Department of the U.S. Air Force, Norton A.F.B., California, 77 p., 11 maps, scale 1:250,000.  
Hanks, T.C., Bucknam, R.C., Lajoie, K.R., and Wallace, R.E., 1984, Modification of wave-cut and faulting-controlled landforms: *Journal of Geophysical Research*, v. 89 (B7), p. 5771-5790.  
Machette, M.N., 1986, History of Quaternary offset and paleoseismicity along the La Jencia fault, central Rio Grande rift, New Mexico: *Geological Society of America Bulletin*, v. 76, p. 259-272.  
\_\_\_\_\_, 1988, Quaternary movement along the La Jencia fault, central New Mexico: U.S. Geological Survey Professional Paper 1440, 81 p.  
\_\_\_\_\_, 1989, Slope-morphometric dating, in Forman, S.L., ed., *Dating methods applicable to Quaternary geologic studies in the western United States: Utah Geological and Mineral Survey Miscellaneous Publication 89-7*, p. 30-42.  
Mayer, L., 1984, Dating Quaternary fault scarps formed in alluvium using morphological parameters: *Quaternary Research*, v. 22, p. 300-313.  
Nash, D.B., 1980, Morphological dating of degraded normal fault scarps: *Journal of Geology*, v. 88, p. 353-360.  
\_\_\_\_\_, 1984, Morphologic dating of fluvial terrace scarps and fault terraces near Yellowstone, Montana: *Geological Society of America Bulletin*, v. 95, p. 1413-1424.  
Pierce, K.L., and Colman, S.M., 1986, Effect of height and orientation (microclimate) on geomorphic degradation rates and processes, late glacial terrace scarps in central Idaho: *Geological Society of America Bulletin*, v. 97, p. 869-885.  
Stewart, J.H., 1983, Cenozoic structure and tectonics of the northern Basin and Range Province, California, Nevada and Utah, in the role of heat in the development of energy and mineral resources in the northern Basin and Range Province: *Geothermal Resources Council, Special Report* 13, p. 25-40.  
Thornbury, W.D., 1969, *Principals of Geomorphology*: John Wiley & Sons, Inc., New York, 594 p.  
Wallace, R.E., 1977, Profiles and ages of young fault scarps, north-central Nevada: *Geological Society of America Bulletin*, v. 88, p. 1267-1281.  
\_\_\_\_\_, 1978, Geometry and rates of change of fault-generated range fronts, north-central Nevada: *U.S. Geological Survey Journal of Research*, v. 6, p. 637-650.  
Zoback, M.L., Anderson, R.E., and Thompson, G.A., 1981, Cainozoic evolution of the state of stress and style of tectonism of the Basin and Range Province of the western United States, in Vines, F.T., and Smith, A.D., eds., *Extensional tectonics associated with convergent plate boundaries: The Royal Society, London*, p. 189-216.

Table 1. Characteristics of young faults in the Elko 1° by 2° quadrangle (See figure 1 for area boundaries)

Orientation	West		Northeast		Southeast	
	Length (km)	Percent	Length (km)	Percent	Length (km)	Percent
90.0 to 80.0°	2.8	0.8	---	---	---	---
79.9 to 70.0°	8.4	2.4	---	---	---	---
69.9 to 60.0°	10.8	3.1	---	---	---	---
59.9 to 50.0°	27.8	8.0	---	---	8.6	1.9
49.9 to 40.0°	49.6	14.3	---	---	6.0	1.3
39.9 to 30.0°	17.6	5.1	12.2	7.9	24.8	5.4
29.9 to 20.0°	86.6	25.0	23.4	15.1	31.2	6.8
19.9 to 10.0°	102.8	29.6	4.0	2.6	95.6	20.8
09.9 to 0.0°	24.2	7.0	32.2	20.7	104.2	22.7
359.9 to 350.0°	12.0	3.5	32.6	21.0	84.4	18.4
349.9 to 340.0°	2.0	0.6	28.4	18.3	52.8	11.5
339.9 to 330.0°	---	---	19.0	12.2	21.0	4.6
329.9 to 320.0°	---	---	---	---	6.8	1.5
319.9 to 310.0°	---	---	---	---	5.0	1.1
309.9 to 300.0°	---	---	3.4	2.2	8.2	1.8
299.9 to 290.0°	---	---	---	---	3.8	0.8
289.9 to 280.0°	2.2	0.6	---	---	7.2	1.6
279.9 to 270.0°	---	---	---	---	---	---
<b>Total (km)</b>	<b>346.8</b>	<b>100.0</b>	<b>155.2</b>	<b>100.0</b>	<b>459.6</b>	<b>100.0</b>
<b>Area (km<sup>2</sup>)</b>	<b>6500</b>	<b>---</b>	<b>5660</b>	<b>---</b>	<b>6450</b>	<b>---</b>
<b>Density (km/km<sup>2</sup>)</b>	<b>0.053</b>	<b>---</b>	<b>0.027</b>	<b>---</b>	<b>0.071</b>	<b>---</b>
<b>Number</b>	<b>60</b>	<b>---</b>	<b>30</b>	<b>---</b>	<b>102</b>	<b>---</b>
<b>Density (no./km<sup>2</sup>)</b>	<b>0.009</b>	<b>---</b>	<b>0.005</b>	<b>---</b>	<b>0.016</b>	<b>---</b>
<b>Mean length (km)</b>	<b>5.8</b>	<b>---</b>	<b>5.2</b>	<b>---</b>	<b>4.5</b>	<b>---</b>

Table 2. General photogeologic and geomorphic criteria used to estimate general ages of piedmont surfaces

Map unit	Age	Depth of dissection	Drainage net morphology	Interfluvial morphology	Geomorphic relations	Typical geomorphic environments	General field criteria
Unit Q3	Holocene (0 to 10 ka)	Shallow to none; generally < 3 m	Predominantly radial from fan apex; channels typically poorly to moderately well defined	Typically poorly defined; bar and sand ridge microtopography commonly on most surfaces	Surfaces cut phluvial shorelines and (or) late Pleistocene glacial moraines	Distal piedmont surfaces; channels and terraces in proximal areas; (proximal) surfaces along some highly active range fronts	Unweathered to slightly weathered; very weak to weak soil development
Unit Q2	Late Pleistocene (10 to 130 ka)	Shallow to moderate; typically 3-6 m	Predominantly distributary; however, some channels head on piedmont; well-defined channels	Typically well defined; surfaces broad and flat with abrupt margins	Surfaces overlain by phluvial shorelines and (or) latest Pleistocene glacial moraines	Proximal to distal piedmont surfaces; some inset terraces	Weakly to moderately well developed soils; interlocking stone pavements
Unit Q1	Early to middle Pleistocene (0.13 to 1.5 Ma)	Moderate to deep; commonly > 10 m	Predominantly subparallel; well-defined channels	Well defined; older interfluvial surfaces commonly irregular and irregularly narrow	Surfaces overlain by phluvial shorelines and (or) Pleistocene glacial moraines	Generally confined to intermediate and proximal piedmont areas	Moderately to very well developed soils; interlocking to highly degraded stone pavements

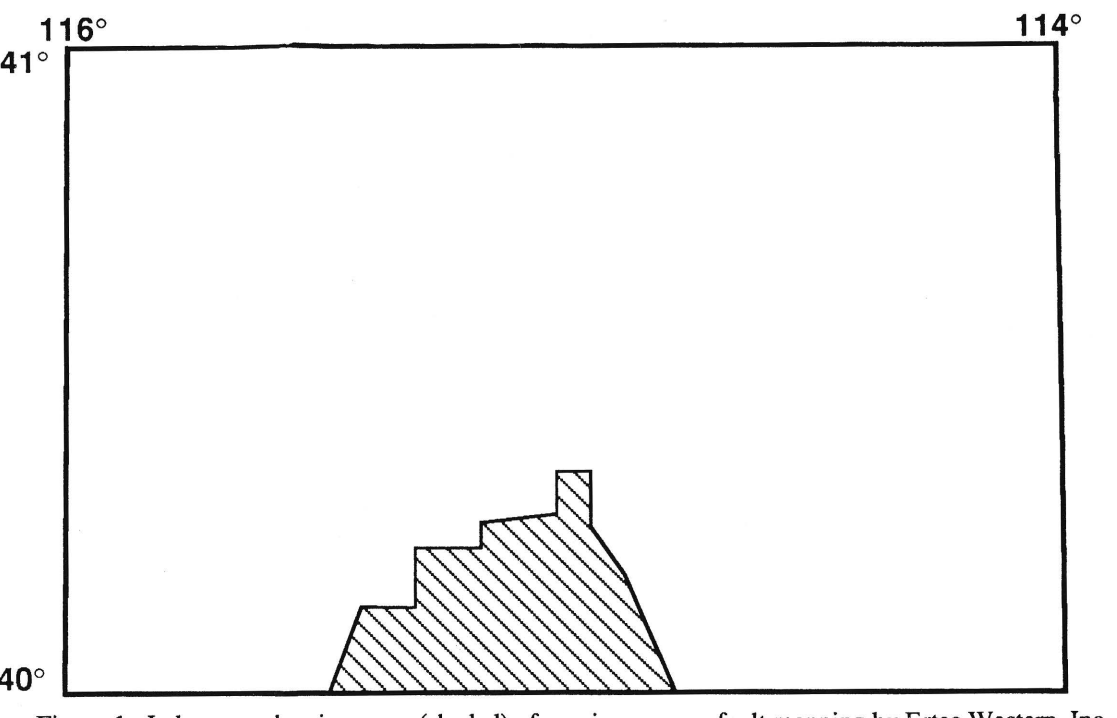


Figure 1. Index map showing areas (shaded) of previous young fault mapping by Ertex Western, Inc. (1981).

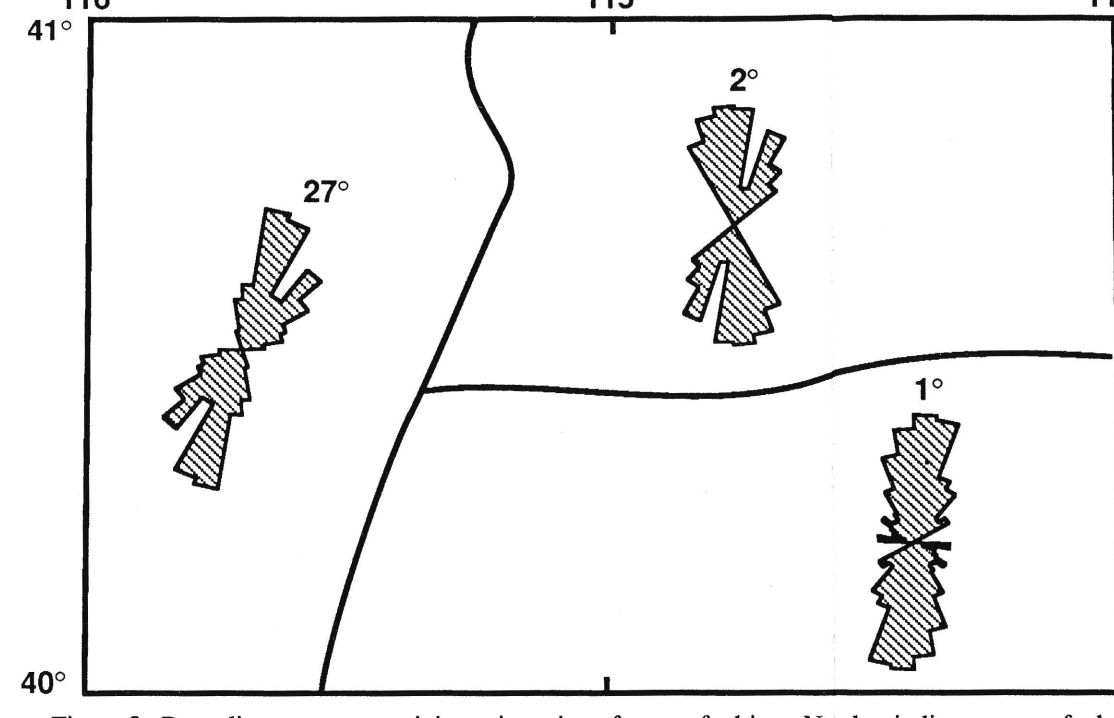


Figure 2. Rose diagrams summarizing orientation of young faulting. Number indicates mean fault trend. See table 1 for data.

RECONNAISSANCE PHOTOGEOLOGIC MAP OF YOUNG FAULTS IN THE ELKO 1° BY 2° QUADRANGLE, NEVADA AND UTAH

By  
John C. Dohrenwend, Bruce A. Schell, and Barry C. Moring  
1991